

Nanoscale

Accepted Manuscript



This is an *Accepted Manuscript*, which has been through the Royal Society of Chemistry peer review process and has been accepted for publication.

Accepted Manuscripts are published online shortly after acceptance, before technical editing, formatting and proof reading. Using this free service, authors can make their results available to the community, in citable form, before we publish the edited article. We will replace this *Accepted Manuscript* with the edited and formatted *Advance Article* as soon as it is available.

You can find more information about *Accepted Manuscripts* in the [Information for Authors](#).

Please note that technical editing may introduce minor changes to the text and/or graphics, which may alter content. The journal's standard [Terms & Conditions](#) and the [Ethical guidelines](#) still apply. In no event shall the Royal Society of Chemistry be held responsible for any errors or omissions in this *Accepted Manuscript* or any consequences arising from the use of any information it contains.

Direct synthesis of graphene 3D-coated Cu nanosilks network for antioxidant transparent conducting electrode

Hongmei Xu ^a, Huachun Wang ^a, Chenping Wu ^a, Na Lin ^{a,e}, Abdul Majid Soomro ^a, Huizhang Guo ^c, Chuan Liu ^d, Xiaodong Yang ^d, Yaping Wu ^{* a}, Duanjun Cai ^{* ab}, and JunYong Kang ^a

^a Fujian Key Laboratory of Semiconductor Materials and Applications, School of Physics and Mechanical & Electrical Engineering, Xiamen University, Xiamen 361005, China. E-mail: ypwu@xmu.edu.cn; dcai@xmu.edu.cn; Fax: +86 592 2187737; Tel: +86 592 2182172

^b Institute of Photonics and Optoelectronics and Department of Electrical Engineering, National Taiwan University, 1, Roosevelt Road, Section 4, Taipei 10617, Taiwan

^c Institute for Building Materials, ETH Zurich, Zurich 8092, Switzerland

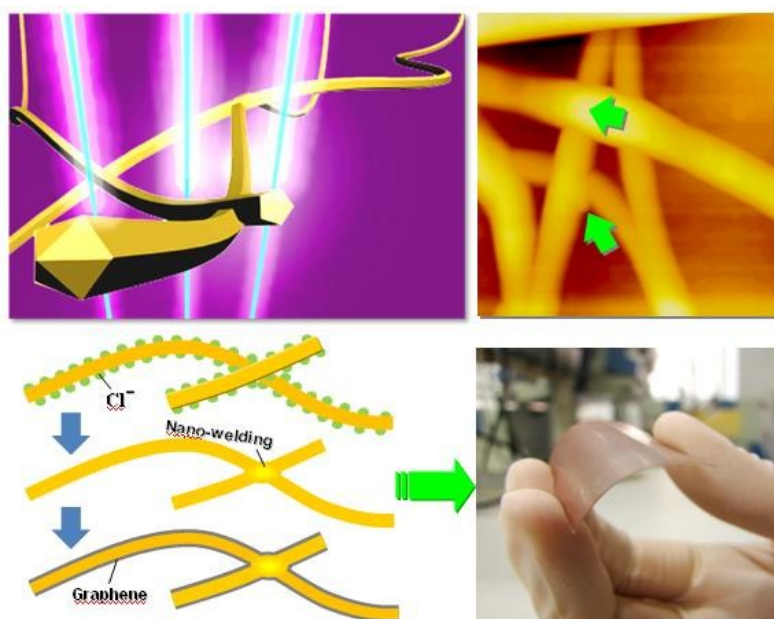
^d State Key Laboratory of Physical Chemistry of Solid Surfaces, College of Chemistry and Chemical Engineering, Xiamen University, Xiamen 361005, China.

^e Xiamen Industrial & Commercial School, Jimei district, Xiamen 361024, China

† Electronic supplementary information (ESI) available: Photographs, transmission spectra, Auger electron spectroscopy (AES) and transmission electron microscopy (TEM) images.

Abstract

Transparent conducting film occupies an important position in various optoelectronic devices. To replace the costly tin-doped indium oxide (ITO), promising materials such as metal nanowires and graphene have been widely concerned. While, a long-pursued goal is to consolidate together these two materials and express their outstanding properties simultaneously. We successfully achieved direct 3D coating of graphene layer on interlacing Cu nanosilks network by low pressure chemical vapor deposition method. High aspect ratio Cu nanosilks (13 nm diameter with 40 μm length) were synthesized through nickel ion catalytic process. Large-size transparent conducting film was successfully fabricated with Cu nanosilks ink by imprint method. A magnetic manipulator equipped with copper capsule was used to produce high Cu vapor pressure on Cu nanosilks and realize graphene 3D-coating. The coated Cu@graphene nanosilks network achieved high transparency, low sheet resistance (41 Ohm/sq at 95% transmittance) and robust antioxidant ability. With this technique, the transfer process of graphene is no longer needed, and the flexible, uniform and high performance transparent conducting film could be fabricated in unlimited size.



Introduction

In recent years, transparent electrodes (TEs) have attracted numerous attentions because of the crucial role playing in the structure of modern optoelectronic devices. TEs which conduct electrical current and allow light to pass through are widely used as the essential component in various optoelectronic devices such as light-emitting diode (LED), photovoltaic cells, photodetectors, solar control windows and touch screens^{1, 2, 3, 4}. In principle, an excellent TE should possess at least low resistance and high transparency as well as physical and chemical stabilities under working. Until now, the most promising TE materials include transparent conductive oxides, carbon nanotubes (CNs), metal nanowire (NW) networks⁵ and graphene⁴. Tin-doped indium oxide (ITO) still takes the place of the best transparent conductive oxide layer with the lowest resistivity on a commercial scale⁶. However, the high price owing to the high cost of indium calls the replacement of ITO by advanced materials. Moreover, the brittleness and low transmittance in blue band strongly limits the application of ITO thin films in flexible⁵ and short-wavelength devices⁷. Nanoscale carbon-based materials⁸ such as graphene have recently come up with exceptionally high mobility and excellent transparency^{9, 10}. While, handicaps of large amount of grain boundaries and wrinkles formed during growth lead to the limitation of graphene sheet resistance¹¹. Hence, the emergence of interlaced metal NW networks⁷ seems to well meet most of the requirements of excellent TEs including good electrical and optical performances, industrial mass synthesis¹² and low cost (the price of Cu is less than 1/10 of ITO). Large area Ag NWs network has been achieved with a sheet resistance of 34 Ohm/sq at 98% transmittance by Leem, D.-S. et al¹³. Guo and his coworkers recently achieved the super-fine Cu nanosilks (NSs) with high optoelectronic performance of 51 Ohm/sq at 93% transmittance and even the application in blue LEDs by accomplishing the ohmic-type contact¹⁴.

In order to prove the wide application of Cu NWs, tests of mechanical and chemical stabilities have been performed by many research groups. Rathmell and his coworkers illustrated that the Cu NW films exhibit very little change (< 10 Ohm/sq) in sheet resistance after 1000 bends by 180° ¹⁵. In contrast, the sheet resistance of ITO films increased by 400 times after just 250 bends. On the other hand, the deterioration test of Cu NSs has been carried out in air for over one month by Guo et al., which definitely showed the rapid influence of the resistance increase by 30 Ohm/sq due to surface oxidation¹⁴. For the issue of oxidation resistance, cupronickel coated Cu NSs have been proposed to prevent them from oxidation¹⁶. Unfortunately, it was also found that the sheet resistance of the Cu@Ni NSs will increase with increasing the Ni concentration. How to improve the stability of Cu NSs without deteriorating or even further enhancing their optoelectronic performance becomes a harsh problem to solve.

This hard nut turns our mind onto the advanced carbon family material - graphene (G), which is a monolayer of two-dimensional (2D) carbon atoms with a cornucopia of enticing properties^{17, 18, 19}. Its excellent properties such as high electrical mobility, high transmittance, high flexibility and also antioxidation provide us a unique candidate for the friendly combination with Cu NSs²⁰. Especially, among various growth methods of graphene, the chemical vapor deposition (CVD) of hydrocarbons precursors on Cu substrate has proven as a versatile technique to achieve large-area, high-quality graphene films from monolayer to multilayer^{21, 22, 23}. Thus, it seems to be feasible to coat graphene directly on Cu NSs, skipping the conventional graphene transfer process, for better solving the conflict between the antioxidation and the improvement of optoelectronic properties.

In this work, we propose a method for achieving direct 3D coating of graphene shell layer on interlacing Cu NS network by low pressure chemical vapor deposition (LPCVD) and

achieving wafer-size fully transparent conducting film. Highly dispersed ultra-long ($> 40 \mu\text{m}$) and super-fine ($\sim 13 \text{ nm}$) Cu NSs have been synthesized through nickel ion catalytic process. The Cu NS ink was imprinted onto 2-inch (Si or sapphire) wafer to form large size TEs through percolation technique. By protection with Cu capsule, the Cu NS network could be protected under Cu atmosphere and remains unmelted at over $700 \text{ }^\circ\text{C}$. Graphene film was then successfully coated on the Cu NS network as a 3D shell layer by using hydrocarbons precursors in a LPCVD system. Owing to the excellent optoelectronic properties of graphene, the coated Cu@G NS TEs achieve simultaneously the higher transparency, lower sheet resistance and robust antioxidant ability. With this technique, free of transfer process, Cu NS network could perfectly combine with graphene for fabricating high performance TEs in unlimited size.

Results and discussion

A route to synthesize superfine Cu NS network

The high-aspect-ratio Cu NSs were synthesized through a solution method with nickel ion catalytic process using a stir heater¹⁴. The as-grown Cu NSs could be well dispersed in hexane solution as an imprinting ink for TE films and show a reddish color, as shown in Fig. 1a. In this way, the ink could be kept stable without oxidation and with good resistivity in TE under ambient for a long time (over 2 months, Fig. S12). Fig. 1c shows the representative SEM image of the Cu NSs, demonstrating the average diameter of $\sim 13 \text{ nm}$ and large length over $40 \mu\text{m}$. They are well dispersed and pure, absent of particle-like structures or aggregated bundles, which ensures the high conductivity in TE films^{24,25}. From the TEM image (Fig. 1d), the individual Cu NS has a uniform diameter of only 13 nm . The corresponding SAED pattern in Fig. 1e shows typical spots of face-centered cubic (*fcc*) structure, indicating the $[1-10]$ growth direction and the $\{111\}$ sidewall planes of the Cu NS. This structure has been proven

to be crucial for a high mechanical strength and high electrical conductivity of Cu NSs²⁶. In our mechanical test, these Cu NSs experience the bending by 180° for 1000 times and remain structurally undamaged and electrically stable (Fig. S13).

The transparent conducting film could then be made from the Cu NS ink by imprint method. The nitrocellulose membrane filtered with Cu NSs through vacuum suction was put face-down on the target substrate such as Si wafer, as shown in Fig. 1b, and then a boat-like stamp was employed to press and roll over the membrane for imprinting the Cu NS film onto the substrate. Via this manner, the TEs in unlimited size or in complicated structure can be easily achieved by multiple imprints and the design of patterned membranes. In present stage, large-size TE with Cu NS network could be uniformly imprinted, e.g., on 2" size semiconductor wafer (Fig. S3) or flexible films (Fig. 4e-f), which well meets the industrial standard of the production of optoelectronic devices.

Copper capsulation against melting of Cu NSs

Based on the imprinted TE film, graphene coating could be carried out using the CVD technique. Typically, the graphene growth by CVD method is performed at about 1000 °C²¹ and the melting point of bulk Cu is 1090 °C²⁷. Hence, one may reasonably choose to perform the coating experiment at 1000 °C. However, the test experiment by heating the Cu NSs up to 1000 °C in vacuum revealed the disaster that the Cu NSs have been seriously melted and broken. This suggests that the actual melting point of Cu in its NS conformation could be far below that of bulk Cu, due to the large surface area of NSs and the significant atom evaporation. In the light of this, we could try to deal with the problem along two lines: one is to reduce the growth temperature T_g of graphene and the other is to increase the melting point T_m of Cu NSs. If these two lines could meet with each other in certain temperature range, the graphene coating could be possible then.

Firstly, the graphene growth on Cu foil at lower temperatures was systematically studied. By using purified methane (CH_4) precursors, the graphene layers can be well grown on Cu substrate at the temperature higher than 900 °C. The typical flower-like graphene flakes begin to nucleate on the surface of Cu foil at a methane flow of 10~20 sccm (Fig. 2a) and as the growth time increases, the flakes gradually coalesce and fully cover the entire Cu surface as a complete graphene film. To examine their property and quality, the graphene film was transferred onto Si surface through the commonly used process with aid of PMMA²⁸ and the Raman spectrum was recorded, as shown in Fig. 2e. One can see that the Raman spectrum reflects the typical monolayer graphene, in which the characteristic 2D peak is sharp and nearly two times the height of the G band. Moreover, the defect-related D peak at about 1350 cm^{-1} is absent, indicating the high quality of the graphene film. However, we found that it becomes difficult to initiate the nucleate of graphene when the growth temperature is lower than 800 °C. As we known, as the temperature decreases the catalytic effect of Cu substrate and the decomposition efficiency of CH_4 rapidly decrease. This is the main reason handicapping the nucleation and growth of graphene at lower temperature. In this regard, several efforts have been made to enhance the carbon concentration and graphene growth rate: (i), by prolonging the annealing time and increasing the hydrogen flow (2~10 sccm), the Cu grain size and orientation can be improved at lower temperature; (ii), the CH_4 flow is continuously increased (20~40 sccm) to enhance the decomposition rate and the carbon concentration on Cu surface; (iii), the pressure of the reaction chamber was slightly increased (8 Torr) by adjusting the rotation speed of turbo pump. Finally, it was found that the CH_4 and the reaction pressures are the most critical factors in pushing the graphene growth at lower temperature. As shown in Fig. 2c-d, when the CH_4 flow rate was increased to 30~40 sccm and the growth time was prolonged to 20~50 min, graphene nucleation and even fully coverage could be successfully achieved on Cu foil at as low as 700 °C. By taking the SEM images of

graphene growth at different time points (Fig. 2f), it can be seen that the flower-like graphene flacks begin to nucleate and ripen gradually as the growth time increases. Finally, the full coverage is accomplished. Raman spectra (Fig. 2e) recorded from the transferred samples confirmed the graphene growth and the crystalline quality. It is believed that 700 °C is near the limiting temperature for the CVD growth of graphene with the gas sources^{29,30}. Hence, we could just stop here and turn to the second line of the research, namely, improving the melting point of Cu NSs.

In order to search the melting point, the Cu NSs were annealed in vacuum at increasing temperatures, 200 °C, 400 °C, 600 °C, 700 °C, 800 °C and 900 °C, respectively. It can be found that below 400 °C the structure of Cu NSs remains stable (Fig. 3a and Fig. S6 in Supporting information) whereas they were melted and aggregated into clusters when the annealing temperature goes beyond 700 °C (Fig. 3b). This result demonstrates that the melting point of Cu NSs should be below 700 °C, lower than the limiting low temperature of graphene growth. At the same time, we observed some light reddish Cu films coating on the inner surface of the quartz tube, indicating the serious evaporation of Cu atoms from the Cu NSs. This evaporation could be attributed to two factors, the very low vapor pressure of Cu above the Cu NSs in vacuum and the long heating time from room temperature up to the annealing temperature. The saturation vapor pressure of Cu at 722 °C has been determined to be about 10^{-8} torr³¹, which is a small value and could be easily fulfilled by introducing foreign Cu source together with NSs. Thus, we propose a method of “Cu capsule”, as shown in Fig. 3d. This Cu capsule could contain the Cu NSs (on Si substrate) in a small space and produce a “Cu” circumstance with higher vapor pressure against melting. On the other hand, a magnetic manipulator (Fig. 3d) was designed to flexibly move the sample with a magnetic slider and to control the annealing time. In details, the sample could be pushed into the heating zone when the annealing temperature is reached and dragged away when the experiment is finished. With

the aid of the Cu capsule and magnetic manipulator, the Cu NSs could perfectly preserve their morphology after annealing at 700 °C for 5 min, as shown in Fig. 3c. The melting point of Cu NSs could even be improved to 800 °C or 900 °C if we carefully shorten the annealing time by using the magnetic manipulator. Up to now, the two temperatures for graphene growth and Cu NS melting have met with each other at least at 700 °C so that the graphene coating could then be carried out.

Direct 3D-coating of graphene shell layer on Cu NSs

The entire process for graphene coating was performed in the following three steps, as shown in the schematics in Fig. 4a. For the as-grown Cu NSs, there exist a layer of surfactants of Cl⁻ ions on the surface of NSs (Fig. S1), which will significantly affect the electrical properties as well as the graphene coating. Therefore, we have to remove the Cl⁻ ions through moderate annealing at about 200 °C for 15 min. After this treatment, the surface of Cu NSs become smooth and the transmittance keeps nearly constant in a broad range from deep-ultraviolet to near-infrared, as shown in the pink line of Fig. 4d. Beside the removal of Cl⁻ surfactants, the nano-welding of interlacing NS junctions was simultaneously accomplished during the annealing, which is critical to get the Cu NSs fused into a conductive network¹⁵. Fig. 3e shows the AFM image of the fused Cu NS network, clearly illustrating the firm welding at the NS junctions. Then, the last step is to coat graphene layers directly onto this Cu NS network in 3D conformation at a higher reaction temperature, e.g., 700 °C in this experiment. For the graphene coating, a high mass flow (30~40 sccm) of CH₄ mixed with H₂ was injected into the reaction chamber, which could enhance entry of CH₄ into the Cu capsule. Within the cavity of Cu capsule, the large inner surface of Cu foil could enhance the CH₄ decomposition rate and provide more C on the sidewall surface of Cu NSs. Thus, the coating of Cu NSs becomes more efficient and faster.

As a result, the graphene was successfully coated on the Cu NS network in 3D conformation, as shown in Fig. 4b. One can see that after coating, the Cu NS network well keeps the NS structure whereas some small particles appear due to slight melting at local junctions connecting several NSs. At these types of junctions, the Cu easily melts into bigger-size particulates. The sidewall surface of Cu NSs remains smooth, indicating that the coated graphene layer adheres tightly following the complicated network surface morphology. The TEM images (Fig. 4c) show the full coverage of graphene layer on the entire Cu NS surface uniformly, which is confirmed by elemental mapping of C [Fig. S18]. We also tried to remove the Cu core of the Cu@G NS by evaporate the Cu at high temperature (900 °C) under vacuum for 15 min. As a result, the Cu NS core has been removed and the graphene shell remains as an individual nanotube, as shown in TEM image in Fig. S17. To further verify the coating of graphene film, Raman spectroscopy was employed to detect the characteristic peaks on selected areas, as marked in the optical image of Fig. 5a. The uncovered bare Si area (blue box) and the Cu NS network (green box) were surveyed for comparison. As shown in Fig. 5b-c, in the bare Si surface only typical characteristic frequencies of Si at 521 cm^{-1} and 964 cm^{-1} (second order peak) can be observed while the representative peaks G, D and 2D for graphene layers clearly appear in the Cu NSs area²². The G band at about 1580 cm^{-1} is related with the sp^2 carbon-carbon bonds and the D and 2D bands are activated by double resonance processes, which reflect the influences by the defects, curvature-induced strains, and disorder in sp^2 -hybridized carbon bonds³². The G peak and the D peak ($\sim 1270 \text{ cm}^{-1}$) are both strong and sharp. This confirms that the graphene uniquely coats on the Cu NS network in a 3D form other than the entire coverage on the whole substrate. Compared with Fig. 2e, the decrease of 2D peak indicates the existence of defects and curvature-induced strains in the multilayer ($\sim 1.8 \text{ nm}$, the inset of Fig. 4c) 3D graphene shell. The C_{1s} spectrum from XPS measurement (Fig. S15) shows a sp^2/sp^3 ratio of about 3.41 ($sp^2 = 77\%$), confirming the domination of the graphene C-C bonding. Moreover, the Raman mapping on the G peak at 1580 cm^{-1} was

performed on a selected individual Cu@G NS (Fig. 5d). The result reveals that the Cu NS has been fully covered by graphene layer after the coating reaction for 5 min, consistent with the TEM results.

High transparency and robust antioxidant ability

The samples of Cu NS network without and with graphene coating were imprinted on quartz glasses, and the transmittance was measured and compared, as plotted in Fig. 4c. It is found that both two samples have a high transmittance in a wide range from 200 nm to 3000 nm. This broad transmission rang strongly suggests their broad applications in optoelectronic devices. Furthermore, the transmittance of Cu@G NSs is significantly enhanced by about 17% after graphene coating, which could be attributed to the surface decoration by graphene layer with the excellent transparency^{28, 33}. Usually, the 2D graphene layer has an obvious absorption at visible band and even below 400 nm. When the graphene is coated on the ultrathin Cu NS in a 3D conformation, the effective absorption area of graphene has been largely reduced and consequently, the short-wavelength transparency exhibits excellent. On the other hand, the sheet resistances of both samples were measured by four-wire resistivity measurement. The result (Fig. S9) showed that the Cu@G NS network possesses a lower resistance of only 41 Ohm/sq at 95% transmittance whereas the resistance of pure Cu NS network is about 51.5 Ohm/sq @ 93%. Because the transport of charges (electrons) is along the Cu NS surface, the graphene coating could effectively improve the mobility of electrons on the Cu-G interface [Fig. S19] and hence, reduces the overall resistance. Since the electron transportation is along the interface, the defects and grain boundaries within the graphene shell layer do not highly involved in the electron transportation and consequently, would not deteriorate the electrical properties.

Finally, the antioxidant ability was examined by heating the sample in air at 200 °C. As shown in Fig. 5e, after heating for 30 min, the plain Cu NS TE has been seriously oxidized experiencing a color change from red to light green, which indicates the formation of CuO³⁴. The SEM image in Fig. 5f shows that the oxidation of Cu surface makes it become extremely rough and the diameter expands (see also the EDS spectrum in Fig. S14, showing the emergence of O after heating). Meanwhile, the resistance has been deteriorated to 554 Ohm/sq after heating for 30 min. In contrast, the Cu@G NS TE well preserves its reddish color as well as the morphology. Most importantly, the resistivity of the Cu@G NS TE remains almost unchanged (Fig. S10), reflecting the robust antioxidant ability under the protection of 3D graphene shell layers. Furthermore, the stability test was carried out under extreme condition of high temperature (85 °C) and high humidity (85%) for 2 h. The results again showed the excellent stability of Cu@G NS TE with constant resistance and transmittance (Fig. S16). Another long time test by keeping the Cu@G NS TE under ambient for 2 months similarly confirms its superstable conductivity suitable for optoelectronic device applications.

Conclusions

In conclusion, we proposed a CVD method for approaching 3D coating of graphene film directly on interlacing Cu NS network as TEs in large size. Ultra-long (> 40 mm) and super-fine (~ 13 nm) Cu NSs have been synthesized via a solution method. Percolation and imprint techniques were proposed to fabricate wafer-size TEs with Cu NS ink on various substrates. The growth temperature of graphene by CVD method was lower to 700 °C and meanwhile, the melting point of Cu NSs was significantly improved up to 700 °C with the protection of Cu capsule. Based on this temperature consistency, graphene film has been successfully coated on the Cu NS network using LPCVD system. This Cu@G NS network achieves high

transmittance, low sheet resistance and strong antioxidant ability owing to the excellent optoelectronic properties of graphene. Via this technique, the outstanding properties of graphene could be more flexibly expressed through the direct coating and tight combination with Cu NSs, which could easily form ohmic contact with various optoelectronic devices.

Experimental

Chemicals:

Copper (II) chloride dihydrate ($\text{CuCl}_2 \cdot \text{H}_2\text{O}$, AR, SCRC), nickel(II) acetylacetonate [$\text{Ni}(\text{acac})_2$, 95%, Strem Chemicals Inc.], hexane (AR, SCRC) oleylamine (80~90%, Acros Organics), hydrogen (99.999%, Linde) and methane (99.999%, Kongfen) were all used as received.

Synthesis of Cu NSs:

A solution method was used to synthesize the Cu NSs, as shown in the following steps: In a typical procedure, 0.8 mmol $\text{CuCl}_2 \cdot \text{H}_2\text{O}$ and 0.4 mmol $\text{Ni}(\text{acac})_2$ were mixed with 10 ml oleylamine in a 50 ml three-necked flask and kept under a flow of high-purity argon at 80 °C for 20 min with strong magnetic stirring. After fully dissolution, the resulting solution was heated up to 175 °C and kept for 9 h. After cooling down to room temperature naturally, excess hexane was added into the red solution to give a red precipitate which was isolated via centrifugation (10000 rpm for 10 min). Cu NS ink was obtained by washing the precipitate with a mixture of hexane and acetone, and then dispersing them into hexane by bath sonication for 10 min.

Fabrication of TEs with Cu NS network:

Thin films were percolated by vacuum filtration and transferred to target substrates such as silicon, sapphire and quartz glass. Firstly, as-synthesized Cu NS ink was filtered onto a nitrocellulose membrane uniformly by vacuum suction to form Cu NS percolation network. Secondly, the nitrocellulose membrane which contacts intimately with Cu NSs was put onto

target substrates and a boat-like stamp was used to imprint under uniform pressure for about 30 s. Finally, the nitrocellulose membrane was peeled off to leave Cu NS network on the substrate and thus, the TE formed on the substrate surface firmly. Moreover, the patterned template could also be put as a mask on the membrane during the vacuum filtration or placed between the membrane and the substrate to produce a patterned TEs structure for specific demands.

Graphene 3D-coating on Cu NS network:

The graphene films were grown on Cu foils (99.8%, uncoated, Alfa Aesar) by using hydrocarbons precursors in a LPCVD system at 1000, 900, 800 and 700 °C. A mixture of CH₄ (10~40 sccm) and H₂ (2~10 sccm) was used for the gas precursors. The Cu substrate was put inside the quartz tube and heated up to 1000 °C under H₂ flow. Then, the Cu foil was annealed at 1000 °C for 20 min under H₂ flow to remove the surface oxide as well as to enlarge the Cu grains. Growth of graphene was initiated by introducing CH₄ after the desired growth temperature was reached and the growth was continued for 5~30 min. After determining the growth condition of graphene on Cu foil, the coating of graphene on Cu NS networks was then processed. The imprinted Cu NS network on a target substrate [e.g. Si (100)] was placed in a Cu capsule and transferred into the quartz tube by a magnetic manipulator. This Cu NS network was first thermally annealed under vacuum (10⁻⁴ Torr) at 200 °C for 20 min to remove the surfactants and achieve the nano-welding of the interlacing NS junctions. Then, the sample was dragged away from the heating zone and the furnace was heated up to 700 °C. When reaching the growth temperature, the capsulated sample was again pushed into the heating zone for 1~5 min and meanwhile, the hydrocarbons precursors (CH₄ and H₂) were injected into the quartz tube for accomplishing the graphene coating. After coating, the sample was immediately pulled out to the room temperature zone for rapid annealing. This coating and annealing process could be repeated for several periods to control the coating thickness of graphene layers.

Characterization:

The as-obtained Cu NSs, Cu@G NS networks, TEs were characterized by means of Normarski optical microscopy (Olympus BX51M), scanning electron microscope (SEM, Hitachi S-4800 scanning electron microscope operated at 20 kV) and transmission electron microscope (TEM, TECNAI F-30 transmission electron microscope operated at 300 kV). The transmittance was tested using a Varian Cary 5000 UV-Vis-NIR spectrophotometer. The sheet resistance was measured using the four-wire resistivity measurement with a Keithley 2450 system. Atomic force microscope (AFM) characterization was carried out using a Veeco Dimension 3100 system in non-contact scanning mode. The Raman spectra and mapping were recorded using a Renishaw InVia Raman Microprobe equipped with a 532-nm laser. The laser spot is about 2 μm in diameter on the sample. The spectrum was taken by averaging over 5 circles.

ACKNOWLEDGMENTS

This work was partly supported by the “973” programs (2012CB619301, 2012CB619304 and 2011CB925600), the NNSF (61204101), the FRFCU (2012121011), and the “863” program (2014AA032608) of China.

Notes and references

- 1 M. Katayama, Tft-lcd technology, *Thin Solid Films*, 1999, **341**, 140-147.
- 2 H. Y. Liu, V. Avrutin, N. Izyumskaya, U. Ozgur and H. Morkoc, Transparent conducting oxides for electrode applications in light emitting and absorbing devices, *Superlattices Microst.*, 2010, **48**, 458-484.
- 3 C. G. Granqvist, Transparent conductors as solar energy materials: A panoramic review, *Sol. Energ. Mat. Sol. C.*, 2007, **91**, 1529-1598.
- 4 L. Gomez De Arco, Y. Zhang, C. W. Schlenker, K. Ryu, M. E. Thompson and C. Zhou, Continuous, highly flexible, and transparent graphene films by chemical vapor deposition for organic photovoltaics, *ACS Nano*, 2010, **4**, 2865-2873.
- 5 Y. Leterrier, L. Médicoa, F. Demarcoa, J.-A. E. Månsona, U. Betzb, M. F. Escolàb, M. K. Olssonb and F. Atamnyb, Mechanical integrity of transparent conductive oxide films for flexible polymer-based displays, *Thin Solid Films*, 2004, **460**, 156-166.
- 6 U. Betz, M. Kharrazi Olsson, J. Marthy, M. F. Escola and F. Atamny, Thin films engineering of indium tin oxide: Large area flat panel displays application., *Surf. Coat. Tech.*, 2006, **200**, 5751-5759.
- 7 H. Wu, L. Hu, M. W. Rowell, D. Kong, J. J. Cha, J. R. McDonough, J. Zhu, Y. Yang, M. D. McGehee and Y. Cui, Electrospun metal nanofiber webs as high-performance transparent electrode, *Nano Lett.*, 2010, **10**, 4242-4248.
- 8 E. M. Doherty, S. De, P. E. Lyons, A. Shmeliov, P. N. Nirmalraj, V. Scardaci, J. Joimel, W. J. Blau, J. J. Boland and J. N. Coleman, The spatial uniformity and electromechanical stability of transparent, conductive films of single walled nanotubes, *Carbon*, 2009, **47**, 2466-2473.
- 9 S. Bae, H. Kim, Y. Lee, X. Xu, J.-S. Park, Y. Zheng, J. Balakrishnan, T. Lei, H. R. Kim, Y. I. Song, Y.-J. Kim, K. S. Kim, B. Özyilmaz, J.-H. Ahn, B. H. Hong and S. Iijima, Roll-to-roll production of 30-inch graphene films for transparent electrodes, *Nat. Nanotec.*, 2010, **5**, 574-578.
- 10 A. Reina, X. Jia, J. Ho, D. Nezich, H. Son, V. Bulovic, M. S. Dresselhaus and J. Kong, Large area, few-layer graphene films on arbitrary substrates by chemical vapor deposition, *Nano Lett.*, 2008, **9**, 30-35.
- 11 U. J. Kim, I. H. Lee, J. J. Bae, S. Lee, G. H. Han, S. J. Chae, F. Güneş, J. H. Choi, C. W. Baik, S. I. Kim, J. M. Kim and Y. H. Lee, Graphene/carbon nanotube hybrid-based transparent 2d optical array, *Adv. Mater.*, 2011, **23**, 3809-3814.
- 12 A. R. Rathmell, S. M. Bergin, Y.-L. Hua, Z.-Y. Li and B. J. Wiley, The growth mechanism of copper nanowires and their properties in flexible, transparent conducting films, *Adv. Mater.*, 2010, **22**, 3558-3563.
- 13 D. S. Leem, A. Edwards, M. Faist, J. Nelson, D. D. C. Bradley and J. C. de Mello, Efficient organic solar cells with solution-processed silver nanowire electrodes, *Adv. Mater.*, 2011, **23**, 4371-4375.
- 14 H. Z. Guo, N. Lin, Y. Z. Chen, Z. W. Wang, Q. S. Xie, T. C. Zheng, N. Gao, S. P. Li, J. Y. Kang, D. J. Cai and D. L. Peng, Copper nanowires as fully transparent conductive electrodes, *Sci. Rep.*, 2013, **3**, 2323.
- 15 A. R. Rathmell and B. J. Wiley, The synthesis and coating of long, thin copper nanowires to make flexible, transparent conducting films on plastic substrates, *Adv. Mater.*, 2011, **23**, 4798-4803.
- 16 A. R. Rathmell, M. Nguyen, M. Chi and B. J. Wiley, Synthesis of oxidation-resistant cupronickel nanowires for transparent conducting nanowire networks, *Nano Lett.*, 2012, **12**, 3193-3199.
- 17 M. I. Katsnelson, Graphene: Carbon in two dimensions, *Mater. Today*, 2006, **10**, 20-27.

- 18 A. K. Geim and K. S. Novoselov, The rise of graphene, *Nat. Mater.*, 2007, **6**, 163-191.
- 19 Y. Zhang, Y. W. Tan, H. L. Stormer and P. Kim, Experimental observation of the
quantum hall effect and berry's phase in graphene, *Nature*, 2005, **438**, 201-204.
- 20 T. H. Ly, D. L. Duong, Q. H. Ta, F. Yao, Q. A. Vu, H. Y. Jeong, S. H. Chae and Y. H.
Lee, Nondestructive characterization of graphene defects, *Adv. Funct. Mater.*, 2013,
23, 5183-5189.
- 21 J. Cho, L. Gao, J. F. Tian, H. L. Cao, W. Wu, Q. K. Yu, E. N. Yitamben, B. Fisher, J.
R. Guest, Y. P. Chen and N. P. Guisinger, Atomic-scale investigation of graphene
grown on cu foil and the effects of thermal annealing, *ACS Nano*, 2011, **5**, 3607-3613.
- 22 D. R. Lenski and M. S. Fuhrer, Raman and optical characterization of multilayer
turbostratic graphene grown via chemical vapor deposition, *J. Appl. Phys.*, 2011, **110**,
013720.
- 23 J. K. Wassei, M. Mecklenburg, J. A. Torres, J. D. Fowler, B. C. Regan, R. B. Kaner
and B. H. Weiller, Chemical vapor deposition of graphene on copper from methane,
ethane and propane: Evidence for bilayer selectivity, *Small*, 2012, **8**, 1415-1422.
- 24 J.-Y. Lee, Connor, S. T., Cui, Y. & Peumans, P., Solution-processed metal nanowire
mesh transparent electrodes., *Nano Lett.*, 2008, **8**, 689-692.
- 25 V. Scardaci, Coull, R., Lyons, P. E., Rickard, D. & Coleman, J. N., Spray deposition of
highly transparent, low-resistance networks of silver nanowires over large areas.,
Small, 2011, **7**, 2621-2628.
- 26 P. Lee, J. Lee, H. Lee, J. Yeo, S. Hong, K. H. Nam, D. Lee, S. S. Lee and S. H. Ko,
Highly stretchable and highly conductive metal electrode by very long metal nanowire
percolation network, *Adv. Mater.*, 2012, **24**, 3326-3332.
- 27 Y. F. Yimin A. Wu, Susannah Speller, Graham L. Creeth, Jerzy T. Sadowski, Kuang
He, Alex W. Robertson, Christopher S. Allen and Jamie H. Warner, Large single
crystals of graphene on melted copper using chemical vapor deposition, *ACS Nano*,
2012, **6**, 5010-5017.
- 28 Z. C. Li, P. Wu, C. X. Wang, X. D. Fan, W. H. Zhang, X. F. Zhai, C. G. Zeng, Z. Y.
Li, J. L. Yang and J. G. Hou, Low-temperature growth of graphene by chemical vapor
deposition using solid and liquid carbon sources, *ACS Nano*, 2011, **5**, 3385-3390.
- 29 Y. Yamazaki, M. Wada, M. Kitamura, M. Katagiri, N. Sakuma, T. Saito, A.
Isobayashi, M. Suzuki, A. Sakata, A. Kajita and T. Sakai, Low-temperature graphene
growth originating at crystalline facets of catalytic metal, *Appl. Phys. Express*, 2012,
5, 025101.
- 30 G. Wang, M. Zhang, Y. Zhu, G. Q. Ding, D. Jiang, Q. L. Guo, S. Liu, X. M. Xie, P. K.
Chu, Z. F. Di and X. Wang, Direct growth of graphene film on germanium substrate,
Sci. Rep., 2013, **3**, 2465.
- 31 R. E. Honig and D. A. Kramer, Vapor pressure data for the solid and liquid elements,
RCA Review 1969, **30**, 285-305.
- 32 L. M. Malard, M. A. Pimenta, G. Dresselhaus and M. S. Dresselhaus, Raman
spectroscopy in graphene, *Phys. Rep.*, 2009, **473**, 51-87.
- 33 S. Bae, H. Kim, Y. Lee, X. Xu, J.-S. Park, Y. Zheng, J. Balakrishnan, T. Lei, H. Ri
Kim, Y. I. Song, Y.-J. Kim, K. S. Kim, B. Ozyilmaz, J.-H. Ahn, B. H. Hong and S.
Iijima, Roll-to-roll production of 30-inch graphene films for transparent electrodes,
Nat. Nanotec., 2010, **5**, 574-578.
- 34 A. O. Musa, T. Akomolafe and M. J. Carter, Production of cuprous oxide, a solar cell
material, by thermal oxidation and a study of its physical and electrical properties, *Sol.
Energ. Mat. Sol. C.*, 1998, **51**, 305-316.

Figure Legends

Fig. 1. Cu NSs synthesized through a catalytic solution method. (a) Photograph of dispersing solution of Cu NS ink in a centrifuge tube, which shows a reddish color. (b) Imprint tools including a boat-like stamp and a filter membrane for fabrication of Cu NS film on wafer size substrate [4" Si(100)]. (c) SEM and (d) TEM images of imprinted Cu NS TEs, respectively. The ultra-long, super-fine and uniform Cu NSs can be observed, which possess an average diameter of ~13 nm. (e) SAED pattern of an individual Cu NS in (d), which demonstrates the *fcc* structure of Cu NS and the growth direction along [1-10].

Fig. 2. Monolayer graphene grown on polycrystalline Cu foils. (a)-(d) SEM images of samples grown at 1000 °C, 900 °C, 800 °C and 700 °C, respectively. (e) A typical Raman spectrum of the graphene layer (grown at 1000 °C) after transferred on Si substrate, which confirms the high-quality graphene monolayer (strong 2D peak) and defect free (absence of D peak). (f) SEM images of graphene growth at different time points.

Fig. 3. Annealing treatment of Cu NS network. (a) and (b) SEM images of Cu NSs after annealing at 200 °C for 1 h and at 700 °C for 5 min, respectively. It is found that the melting point of Cu NSs is around 700 °C, much lower than that of bulk Cu (1085 °C). (c) SEM image of Cu NSs capsulated by Cu foil pocket after annealing at 700 °C for 5min. The Cu capsule could well protect the Cu NSs from melting. (d) Schematic of the LPCVD system equipped with magnetic manipulator and Cu capsule. (e) AFM image of Cu@G NS network. It shows that the nano-welding junctions firmly connect interlacing NSs into conductive network and the graphene coating is in a 3D conformation.

Fig. 4. Direct 3D-coating of graphene shell layer on Cu NS network. (a) Schematics of the 3D-coating processes of graphene on Cu NS networks. (b) SEM image of Cu NSs after graphene 3D-coating. The graphene-coated Cu NSs well preserve the conformation of interlacing network. (c) Bright-field TEM image of individual Cu@G NS. The inset shows the close coating of graphene layer on the sidewall surface. (d) Optical transmittance spectra of the Cu NS TEs on quartz substrate before (pink) and after (green) graphene coating. The transmittance is improved due to the excellent transparency of the graphene shell layer. (e) and (f) Photographs of Cu NS ink filled in an injector and flexible TE of Cu NS film on PET paper, respectively.

Fig. 5. Structure and antioxidation test of Cu@G NS network. (a) Optical image of Cu@G NS film on Si substrate. The blue and green rectangular boxes mark the bare Si area and the Cu@G NSs, respectively. (b) and (c) Raman spectra of bare Si substrate and Cu@G NSs, respectively, recorded from correspondingly marked areas in (a). They confirm that the graphene layer uniquely coats on the Cu NS network. The inset of (b) shows the introduction of field iris diaphragm for the focus on Si surface. (d) Optical image and color-coded Raman mapping (inset) of a single Cu NS at the G peak, which suggests that the entire Cu NS has been fully coated by graphene. (e) Photographs of Cu NS and Cu@G NS TEs on quartz glass before and after heating in air at 200 °C for 30 min. These demonstrate the strong antioxidant ability of the Cu@G NS network with stable resistivity. (f) SEM images of Cu@G NS and Cu NS TEs after heating. The oxidation of Cu makes the NS sidewall surface seriously rough.

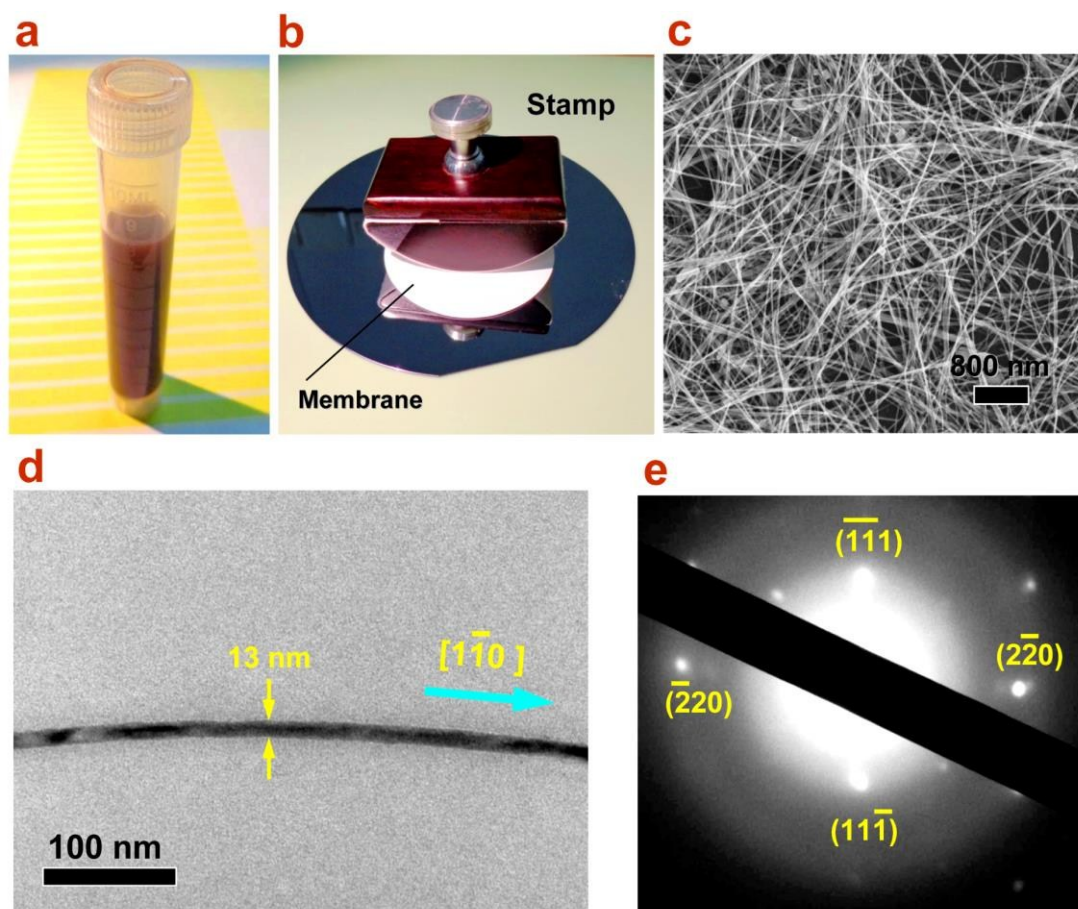


FIG 1. H. M. Xu et al.

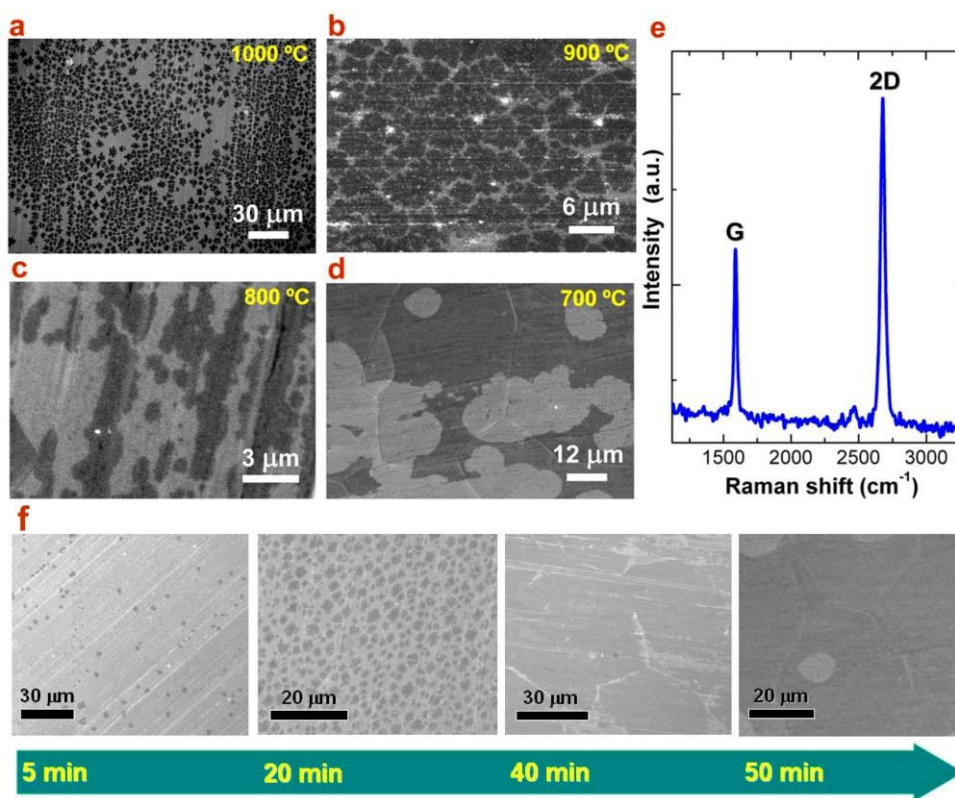


FIG 2. H. M. Xu et al.

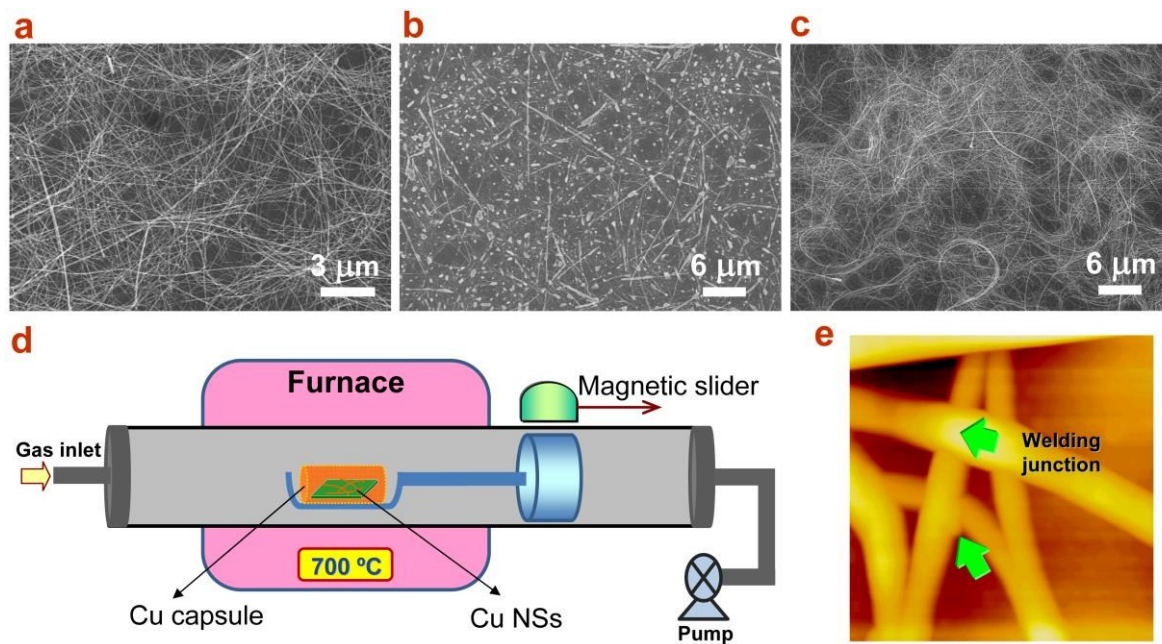


FIG 3. H. M. Xu et al.

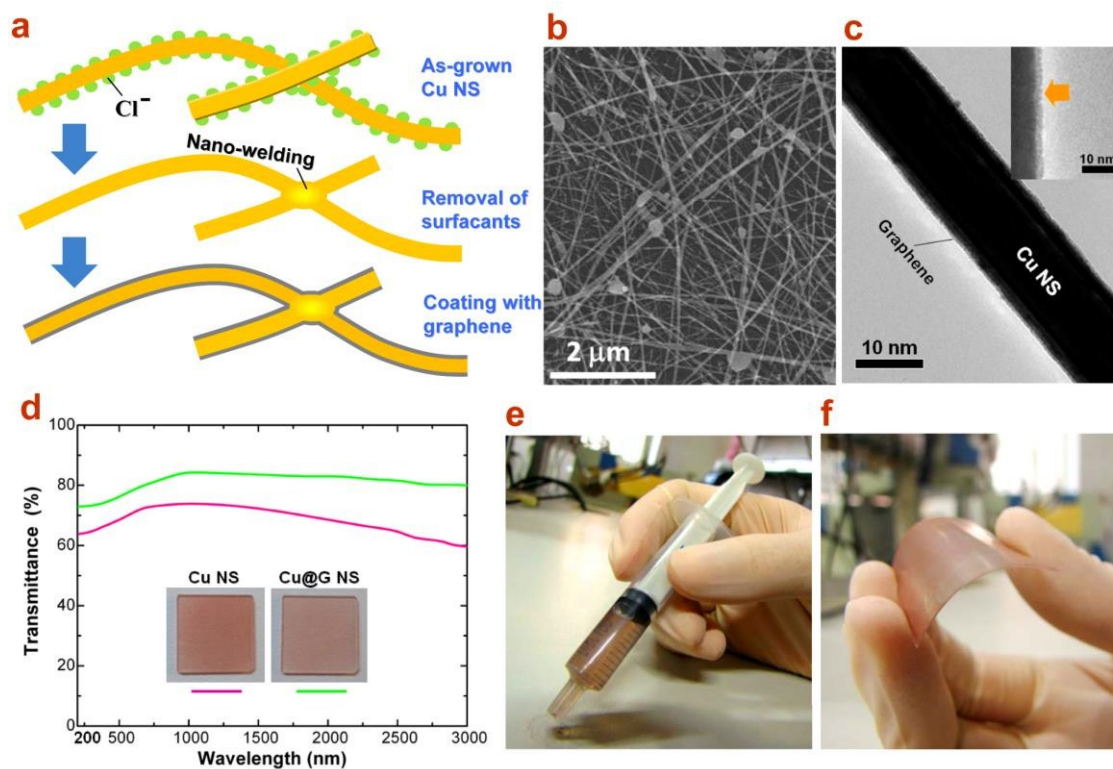


FIG 4. H. M. Xu et al.

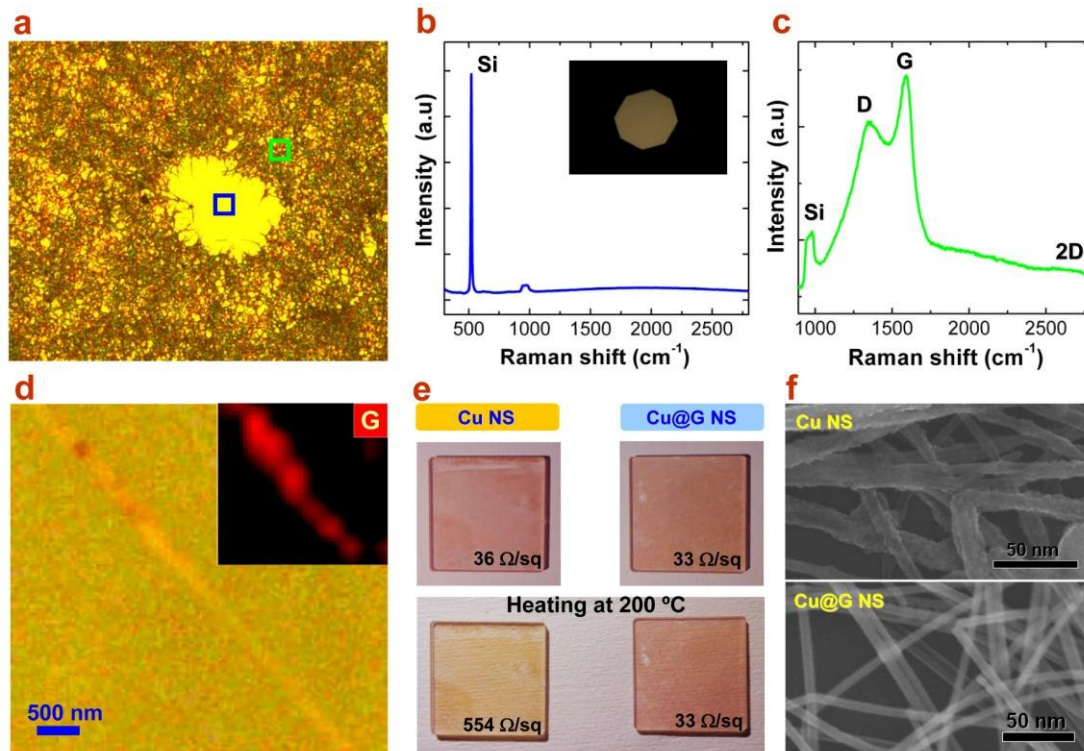


FIG 5. H. M. Xu et al.